International Journal of Heat and Fluid Flow 30 (2009) 814–822

Contents lists available at ScienceDirect

International Journal of Heat and Fluid Flow

journal homepage: www.elsevier.com/locate/ijhff

Friction factor in micropipe gas flow under laminar, transition and turbulent flow regime

G.P. Celata [a,*], M. Lorenzini [b], G.L. Morini [b], G. Zummo [a]

[a] ENEA, Istituto di Termofluidodinamica, 00060 S.M. Galeria, Roma, Italy
[b] DIENCA, Università di Bologna, Viale Risorgimento 2, 40136 Bologna, Italy

ARTICLE INFO

Article history:
Received 17 October 2008
Received in revised form 26 February 2009
Accepted 28 February 2009
Available online 1 April 2009

Keywords:
Microscale
Friction factor
Gas flow
Laminar flow
Turbulent flow

ABSTRACT

The present work deals with the compressible flow of nitrogen gas inside microtubes ranging from 30 to 500 μm and with different values of the surface roughness (<1%), for different flow regimes. The first part of the work is devoted to a benchmark of friction factor data obtained at DIENCA (University of Bologna) and the ENEA laboratories, using fused silica pipes of 50 and 100 μm. Data overlapping is excellent thus evidencing how the agreement of the experimental data with the classic theory is independent of the measurement system. The second part of the work demonstrates that classic correlations can predict friction factor in laminar flow without revealing any evident influence of the surface roughness. The laminar-to-turbulent transition starts for Reynolds number not lower than 2000 for smooth pipes, while tending to larger values (3200–4500) for rough pipes. Anyway, contrarily to other available results, no dependence of the critical Reynolds number on the *L/D* has been observed. Changes in the flow regime have been found of the sharp and smooth type, like for larger pipes; smooth transition looks typical of smooth pipes while the sharp transition in the flow pattern is associated with rough pipes. In the fully developed turbulent regime, obtained for both smooth and rough pipes, an agreement between experimental data and the Blasius correlation has been verified for smooth pipes, while for rough pipes the agreement with predictions given by the Colebrook equation is rather modest.

1. Introduction

A number of studies on liquid and gas fluid flow have been carried out over the last years. Experimental results are more and more in agreement with the predictions provided by classical theories. This can be explained with the improvement in the micromanufacturing techniques which have allowed a better control of surface roughness and of the geometric characteristics of conduits. Nonetheless, we still believe systematic studies are necessary both to provide a coherent treatment of the matter, and to have a better insight in some fluid dynamics aspects, such as the laminar-to-turbulent transition. Validity of conventional correlations for the incipient and completely developed turbulent flow has to be ascertained as this matter is still debated. Even the independence of the friction factors on roughness in the laminar regime has been recently questioned by Tang et al. (2007) and Vijayalakshmi et al. (2009) found results in discrepancy with the classical correlations in the turbulent regime, so more data are needed to contribute to either theory.

Laminar-to-turbulent transition has been analysed by Morini (2004a, 2004b) and Hetsroni et al. (2005). The transition, in microgeometries, would seem to occur at critical Reynolds number ranging from 70 (Peng and Peterson, 1996) up to 10,000 (Stanley et al., 1997). This wide range of the critical Reynolds number has spinned further works. Wu and Little (1983) were the first to measure the friction factor in rectangular and trapezoidal glass and silica microchannels with different gases (N_2, H_2, Ar); measured friction factors are higher (10–30%) than those predicted by the classical theory. Authors have argued about the role of the relative surface roughness in the transition, found to occur for Reynolds number between 100 and 3000. Acosta et al. (1985) have presented an analysis of friction factors for isothermal gas flow in rectangular microchannels having a quite low aspect ratio. Experimental tests have shown a critical Reynolds number of 2770, as reported by Obot (2002), i.e., similar to those typical of the conventional geometries. Choi et al. (1991) have determined the friction factor for the fully developed laminar flow of nitrogen in microtubes with diameter of 3, 7, 10, 53 and 81 μm, for Reynolds number varying between 30 and 20,000. These data exhibit a reduction of the critical Reynolds number with the hydraulic diameter; in particular, the transition takes place at $Re = 2000$ for a circular micropipe with a hydraulic diameter of 53 μm, and at $Re = 500$ for a tube of 9.7 μm diameter. Yu et al. (1995) have analysed nitrogen and water

* Corresponding author. Tel.: +39 06 3048 3905; fax: +39 06 3048 3026.
E-mail address: celata@enea.it (G.P. Celata).

0142-727X/$ - see front matter © 2009 Elsevier Inc. All rights reserved.
doi:10.1016/j.ijheatfluidflow.2009.02.015

Nomenclature

A	cross section, m^2
D	diameter, m
f	friction factor (Darcy-Weisbach), –
FS	full scale, –
L	length, m
Γ	mass flow-rate, kg s^{-1}
Ma	Mach number, –
p	pressure, Pa
Po	Poiseuille number, –
R	gas constant, J kg^{-1} K^{-1}
Re	Reynolds number, –
Re^*	Friction Reynolds number, –
T	temperature, °C

Greek letters

Δ	difference, –
ε	roughness, m
μ	Dynamic viscosity, Pa s
ρ	density, Kg m^{-3}

Subscripts

c	critical
h	hydraulic
ex	exit
i	inlet
n	net
no	nominal
o	outlet

flows along silica microtubes with diameters of 52, 102 and 191 μm for Reynolds numbers ranging from 250 to 20,000. They found that transition takes place for Reynolds number between 1700 and 6000, i.e., accordingly to predictions obtained from the theory of continuum. Stanley et al. (1997) have carried out experiments on liquid and gas flows in rectangular microchannels with hydraulic diameters between 56 and 260 μm. For nitrogen flow the transition has been detected for Reynolds numbers between 1500 and 2000 when the hydraulic diameter of the tube is larger than 150 μm. Li et al. (1999), testing gas flow in microtubes reported a critical Reynolds number of 2300 up to 3000. In a later work, Li et al. (2000), they found transition to occur at Reynolds numbers ranging between 1700 and 2000. Yang et al. (2000), testing air, water and R-134a flow in microtubes have found transition to occur at Reynolds numbers between 1200 and 3800. The range of the critical Reynolds number increases as the pipe diameter decreases, the functional dependence on the diameter being more pronounced for water than for air. Faghri and Turner (2003) have studied the effect of the relative roughness in microchannels obtained from ⟨100⟩ (which generates a trapezoidal cross section) and ⟨101⟩ (which produces rectangular cross sections) silicon wafer. They have tested nitrogen and helium flows for different relative roughness values, verifying that the friction factor is independent of the relative roughness as long as the latter is lower than 6%, these results being completely in accordance with the classical theory. Tang and He (2004) measured the friction factor for nitrogen flows in fused silica pipes and square duct microchannels with diameter ranging between 50 and 201 μm. Although the authors found the good agreement between experimental data and classical theory predictions, for the smallest pipe diameter compressibility, roughness and rarefactions effects could not be neglected any longer. Laminar-to-turbulent transition has been detected for Re = 1900–2500. Kohl et al. (2005) have carried out experiments of water and air flows in rectangular microchannels with hydraulic diameters ranging between 24.9 and 99.8 μm, finding again a good agreement between their laminar flow data and the conventional theory and no anticipated transition. However, they reported that when compressibility effects become significant the critical Reynolds number can be affected by the L/D ratio. For air they found critical Reynolds numbers ranging between 2300 and 6000, the value being dependent on L/D. This behaviour has been explained taking into account the relevant acceleration inside the microtube, as theoretically predicted by Kurokawa and Morikawa (1986), and by Schwartz (1987).

Tang et al. (2007) investigated among others the effect of roughness on friction factor in rough steel microtubes of circular shape and diameter of 300, 260, 172, and 119 μm, concluding that for these the high roughness (fro, 2.3% up to 5.9%) bring about an increase in the friction factor in the laminar regime even for low Reynolds numbers, contrary to what they find in fused silica tubes of circular and square cross-section, where roughness is well below 1%. They do not give precise data for the values of the critical Reynolds number, but the plots show values around 2000–2400, so the data conform to classical predictions.

Recently, Vijayalakshmi et al. (2009) investigated transition to turbulence in smooth (roughness less than 0.1%) trapezoidal channels with hydraulic diameters between 60.5 and 211 μm and nitrogen and water flows, in an attempt to separate deviations from the Poiseuille curve due compressibility effects (where applicable) from actual transition to turbulence and finding that the latter occurs in the range of Reynolds numbers between 1600 and 2300. Their data for the transitional regime, however fall significantly below the classical predictions.

From the above analysis of the literature, which is summarised in Table 1, we can conclude that the flow behaviour in the transition region is still an open question for microchannels. Because of the highest velocities and the corresponding Reynolds numbers, this matter is more relevant for microchannel gas flow. Likewise, the friction factor in laminar and turbulent flow calls for further experimental testing to ascertain whether classical correlations can provide accurate predictions or not. In this respect, it is also advisable that different research groups perform experiments on the same microtubes using different measurement techniques and fluids, in order to verify the coherence of data obtained in the respective laboratories. With this aim, the first part of the work is dedicated to the comparison of data carried out at the laboratories of the Institute of Thermal Fluid Dynamics of ENEA (Rome, Italy) and at the microthermofluidics laboratory of the University of Bologna, Italy (DIENCA). In the two experiments the same fused silica micropipes have been tested in laminar gas flow, using two different facilities and different gases. In the second part of the work different tubes of different material have been tested in order to analyse the behaviour in the transition and in the turbulent flow region, comparing the results with predictions obtained using classical correlations.

2. The experimental facilities

Experimental facilities used in the benchmark have been schematically drawn in Fig. 1. The ENEA facility (Fig. 1a) is made of a pressurized tank of helium the pressure of which is reduced to about 20 bar before the fluid is filtered (0.5 μm filter): a micro

Table 1
Works on laminar-to-turbulent transition for gas flows in microchannels.

Authors	D_h (μm)	Section and fluid	ε/D_h (%)	L/D_h	Re_{cr}
Wu and Little (1983)	55.8–83.1	[b,c]N_2,H_2,Ar	20–30	100–720	1000–3000
Acosta et al. (1985)	953	[b]N_2	0.13–5.2	–	2770
Choi et al. (1991)	3.0–81.2	[a]N_2	0.02–1.16	640–8100	2000–2300
Yu et al. (1995)	19–102	[a]N_2	<0.03	–	1700–6000
Stanley et al. (1997)	56–260	[b]N_2	n/a	–	1500–2000
Li et al. (1999)	79.9–166.3	[a]N_2	0.1–3.9	145–715	2300–3000
Li et al. (2000)	79.9–179.8	[a]N_2	0.1–3.9	690–3984	1700–2000
Yang et al. (2000)	173–4010	[a]Air	NA	690–3984	1200–3800
Faghri and Turner (2003)	9.7–46.6	[b,c]N_2, He	0.1–6	263–5717	2000–2500
Tang and He (2004)	50–201	[a,b]N_2	0.1–5	498–995	1900–2500
Kohl et al. (2005)	24.9–99.8	[b]Air	0.29–1.3	220–533	2300–6000
Kandlikar et al. (2005)	684–953	[b]Air	7.35–11	104–146	800
Morini et al. (2006)	133–751	[a]N_2	1–5	575–3750	1800–2900
Morini et al. (2007)	100–300	[a]N_2	≈0	166–5000	2100–6000
Tang et al. (2007)	50–300	[a,b]N_2, He	0.1–5	333–3000	1800–2700
Vijayalakshmi K. (2009)	60.5–211	[c]N_2	>0.1	246–860	1600–2300
Hrnjak and Tu (2007)	69.5–304.7	[b]R134a(v)	0.45–1.25	315–691	1500–2500

[a] Circular cross-section.
[b] Rectangular cross-section.
[c] Trapezoidal cross-section.

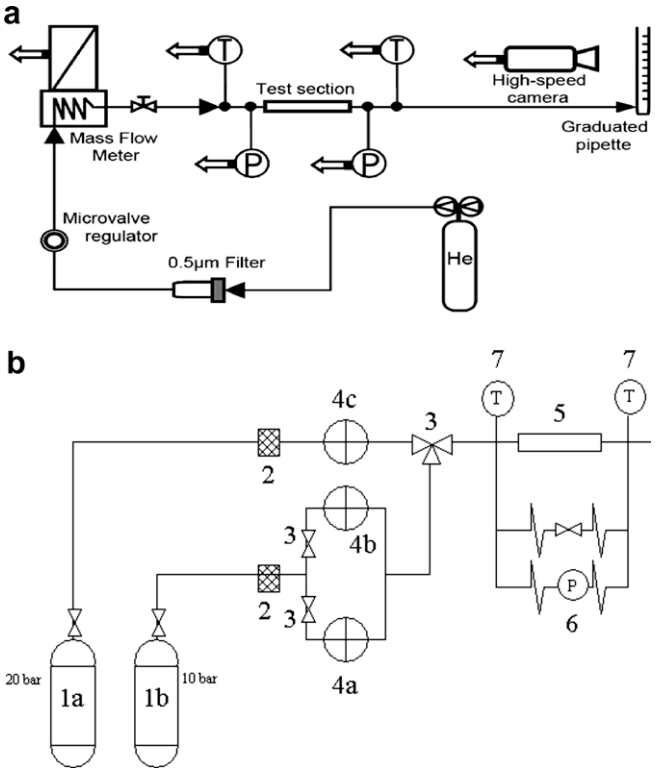

Fig. 1. Sketches of ENEA (a) and DIENCA (1b) facilities.

valve regulator adjusts the pressure to the value chosen for the test. The pressure measurements are taken just upstream and downstream of the test section using an absolute pressure transducer (Druck PTX100/IS, 0–35 bar) and a differential one (Rosemount 1151DP, 0–6.85 bar). Temperatures are measured using K-type thermocouples. For the measurement of the gas flow-rate two methods are used. For gas flow-rate higher than 0.5 mg/min a calibrated pipette is used: a drop of water and soap solution is placed inside the pipette in order to create a meniscus the position of which can be detected by a high-speed camera. From the pipette diameter and the meniscus velocity it is possible to evaluate the volumetric gas flow rate. The gas is then directly vented to the atmosphere. For smaller gas flow-rates a flow-rate transducer is used (Bronkhorst EL-Flow, 0–5 nml/min).

The schematic of the facility used at the University of Bologna is plotted in Fig. 1b. Nitrogen is stored inside two different tanks, with exit pressure at 20 and 10 bar, respectively (1a–1b). Two 7 μm-filters (2, Ham-let) are placed on each line before the flow-meters to prevent possible obstruction of the test section with impurities. Ball-valves (3) are used to select the appropriate gas line and flow-meter, as three Bronkhorst EL-Flow E7000 are used, operating in the following ranges: 0–5000 nml/min (4a), 0–500 nml/min (4b) and 0–50 nml/min (4c). Flow-meters can also impose the mass flow-rate via a PC controlled needle valve, thus allowing an indirect pressure regulation at the microtube inlet. Gas flow enters the test section (5), upstream of which the pressure tap is located. Test section up to 100 cm long can be accommodated in the facility, with a maximum external diameter of 1/16 in. At the microtube exit the gas is vented to the atmosphere. A differential pressure transducer (6, Validyne DP15) is used to measure the pressure drop across the test section. The pressure transducer has an interchangeable sensor in order to ensure accurate measurements in the whole range of pressures. The temperature upstream and downstream the test section is measured using K-type thermocouples (7): from gas temperature and pressure measurements it is possible to evaluate the gas density upstream and downstream the test section.

Seven commercial (Upchurch Inc.) microtubes have been tested: three fused silica micropipes (FS), two PEEK covered fused silica micropipes (PS), and two stainless steel micropipes (SS). The main geometric characteristics of the test sections are summarized in Table 2. The inner diameter of each micropipe (at the front cross section) has been verified using a SEM (JEOL JSM 5200). Typical

Table 2
Main geometrical characteristics of the tested pipes.

Pipe name	D_{no} (μm)	D (μm)	L (cm)	L/D	ε/D (%)	Re
FS1	20	29.9	5.05	1689	~0	70–1050
FS2	50	51.4	4.90	953	~0	50–2760
FS3	100	100.0	10.00	1000	~0	20–4050
PS1	25	26.1	5.00	1916	~0	90–750
PS2	50	52.2	5.00	958	~0	30–3034
SS1	250	275.0	20.00	727	1.0	400–9500
SS2	500	508.0	30.00	591	0.8	1800–14,500

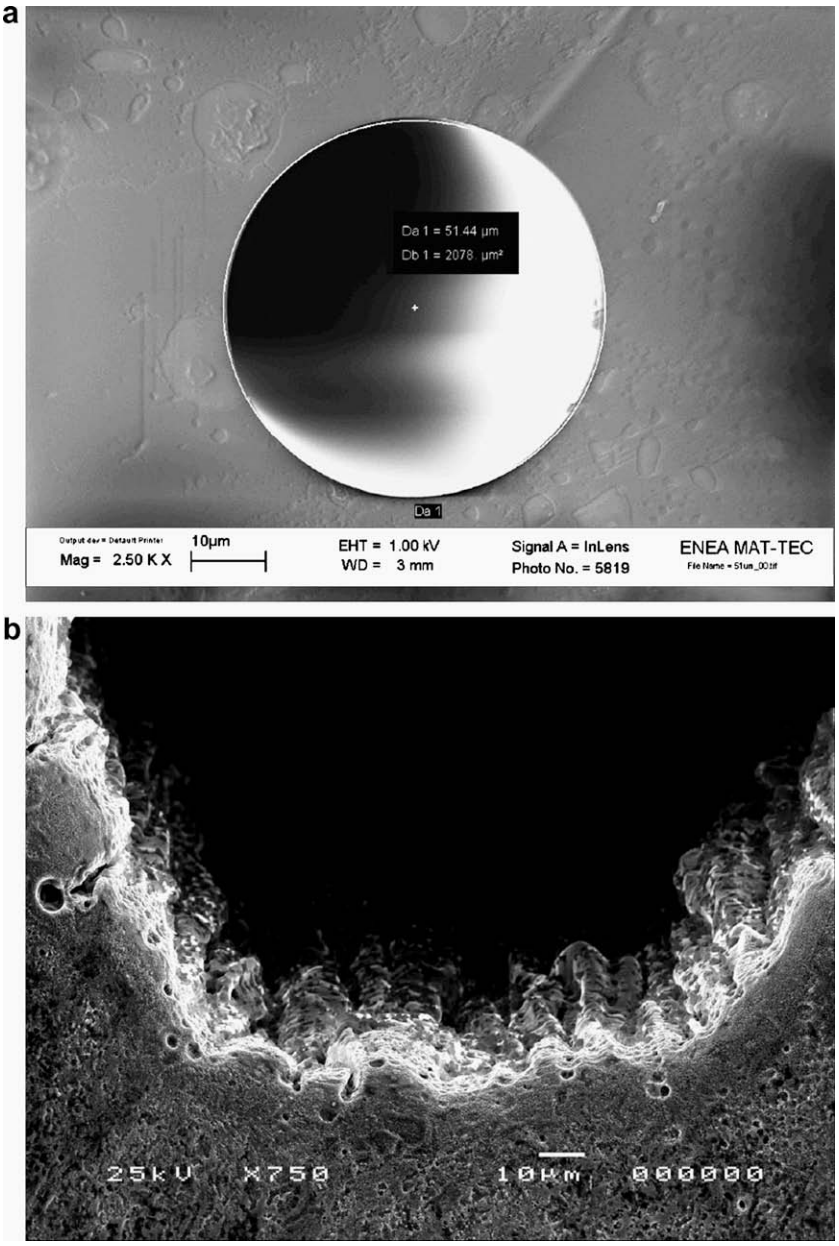

Fig. 2. SEM images of pipe cross section for fused silica (FS2, a) and stainless steel (SS1, b) pipes.

images of a fused silica pipe (FS1) and a stainless steel pipe (SS1) are shown in Fig. 2. Pictures confirm that fused silica pipes can be assumed to be smooth. Conversely, stainless steel pipes are characterized by a strongly irregular contour. SEM images of each tube have been used to verify the inner diameter and the average height of the asperities.

A large difference between the nominal diameter (D_{no}) and the actual one (D), which is up to about 50% (FS1), has been measured. Actual diameters determined from the analysis of SEM images of pipes are shown in Table 2. Measurements of the diameter were only taken at one cross-section per tube; as the diameters yield results which agree quite well with the theoretical predictions for laminar flows using those diameters, it can be assumed with reasonable confidence that the deviation along the axis of the diameter from the measured value is modest and the latter is representative of the actual geometry. The average roughness (ε) for stainless steel pipes is 3–4 µm, while the relative roughness (ε/D) ranges between 0.8% and 1%.

3. Experimental uncertainty and data analysis

For channels with $L \gg D$ the flow can be considered as isothermal, owing to the large surface available to heat transfer. As current test sections are characterized by $L/D > 600$ this approximation can be considered as valid. An equation for the calculation of the friction factor for a non-compressible isothermal flow in a duct is proposed by Shapiro (1953):

$$f = \frac{D}{L}\left[\left(\frac{1-\left(1-\frac{\Delta p_n}{p_i}\right)^2}{\left(\frac{\Gamma\sqrt{RT}}{\Delta p_i}\right)^2}\right) - 2ln\left(\frac{1}{1-\frac{\Delta p_n}{p_i}}\right)\right] \quad (1)$$

The net pressure drop is deduced from the differential pressure measurement, as explained in other works (Morini et al., 2006, 2007). For compressible viscous flow the Reynolds number could vary along the test pipe if the volumetric flow was imposed. In the present work we refer to the Reynolds number defined as:

$$R = \frac{\Gamma D}{A\mu} \tag{2}$$

For an isothermal flow the Reynolds number defined in Eq. (2) is constant along the microtube.

In order to evaluate the accuracy of the measurements the uncertainty associated with instruments used at DIENCA are reported in Table 3. For ENEA measurements this piece of information can be found in Celata et al. (2006).

The uncertainty in the evaluation of f and Re can be estimated after Moffat (1988), starting from the uncertainty associated with the measurement of the single parameters involved in the calculation of f and Re, i.e., p, D, L,, etc. This procedure is thoroughly described by the authors in Lorenzini et al. (2007), which the reader is referred to. The uncertainty associated with the measurement of the tube diameter has the largest weight in the total uncertainty. In the present works the uncertainty in the tube diameter, measured with a SEM, is a maximum of ±2%, while that associated with the pipe length is less than ±0.8%.

4. Results and discussion

As already stated the first part of this work is related to the benchmark carried out at ENEA and at DIENCA to verify measurements performed with the same test sections in different facilities. Further tests have been carried out at DIENCA to ascertain the possibility for laminar and turbulent gas flows to be predicted using conventional pipe laws. To this purpose experimental data are plotted using the Moody diagram, where the Poiseuille law is drawn ($f = 64/Re$, $Re < 2000$, circular pipe) and the Blasius law ($f = 0.316/Re^{0.25}$, smooth pipe, turbulent flow) are plotted. The Poiseuille law is drawn with a continuous line, while the Blasius law is represented by a dot-dashed line

4.1. Laminar regime

Experimental results obtained at ENEA (using helium) and at DIENCA (using nitrogen) for microtubes FS2 and FS3 are plotted in Fig. 3, where for readability error bars are omitted (however uncertainties are within ±10%). The two series of experimental results are quite in a good agreement for the laminar regime. Fig. 3a shows a slight scatter (DIENCA data) for $Re < 50$, which is due to tests performed at the lower end the flow meter working range. All in all, the agreement of the data with the Poiseuille law looks excellent. If possible, Fig. 3b shows even a better agreement in the laminar region, while in the turbulent regime tests carried out at DIENCA are closer to the predictions of Blasius. The transition mode for the FS3 pipe has been found smooth and bounded by critical Reynolds numbers between 2200 and 2500. In a previous work (Morini et al. (2007)) the Poiseuille number was plotted as a function of the average Mach number, and it was shown that at some value corresponding to a change in the flow regime the Poiseuille number starts to increase steeply without any appreciable increase in the Mach number. The corresponding value of the Reynolds number is taken as critical value.

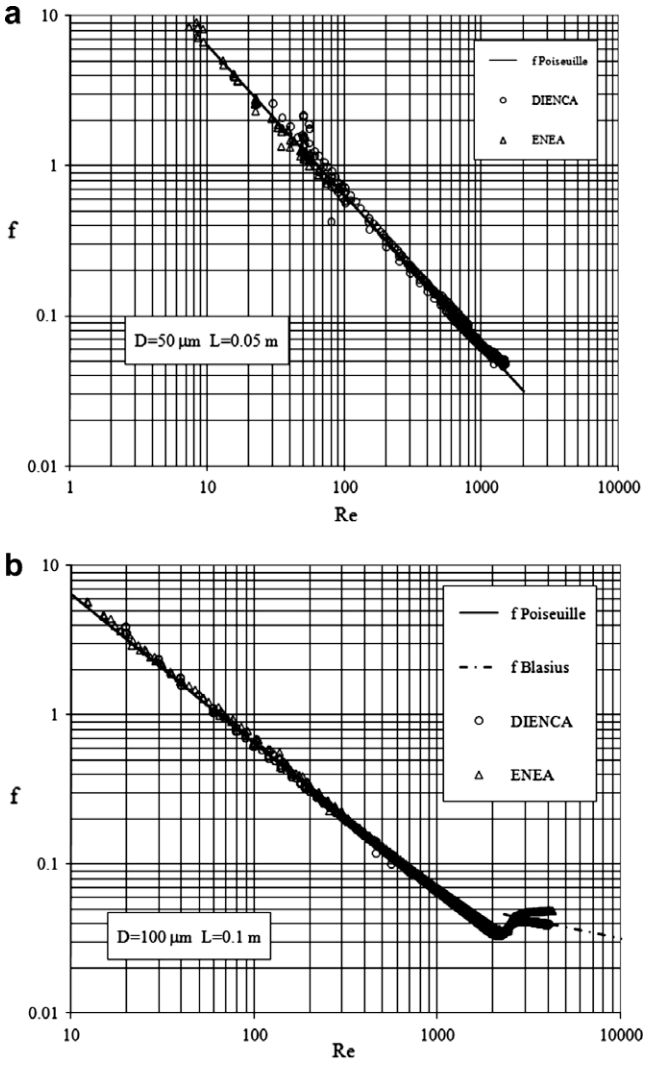

Fig. 3. Friction factor for microtubes FS2 (a) and FS3(b) obtained at ENEA (helium) and at DIENCA (nitrogen).

Fig. 4 shows the friction factor obtained for the fused silica pipe FS1 using the nominal diameter provided by the manufacturer, i.e., 20 μm. We can observe how the friction factor would be largely overestimated by the Poiseuille law (laminar regime). Conversely, using the pipe diameter obtained from SEM images, i.e., $D = 29.2$ μm, the friction factor is in excellent agreement with the theoretical prediction. This further testifies the importance to accomplish accurate measurements of the pipe diameter in the

Table 3
Instrumentation and accuracy at DIENCA.

Reference	Sensor	Field	Uncertainty
(4a)	Flow meter	0–5000 (nml/min)	±0.6% FS
(4b)	Flow meter	0–500 (nml/min)	±0.5% FS
(4c)	Flow meter	0–50 (nml/min)	±0.45% FS
(6)	Differential pressure transducer	0–35 (kPa) 0–86 (kPa) 0–220 (kPa) 0–860 (kPa) 0–1440 (kPa)	±0.5% FS
(7)	Thermocouple	0–200 (°C)	±0.25% FS

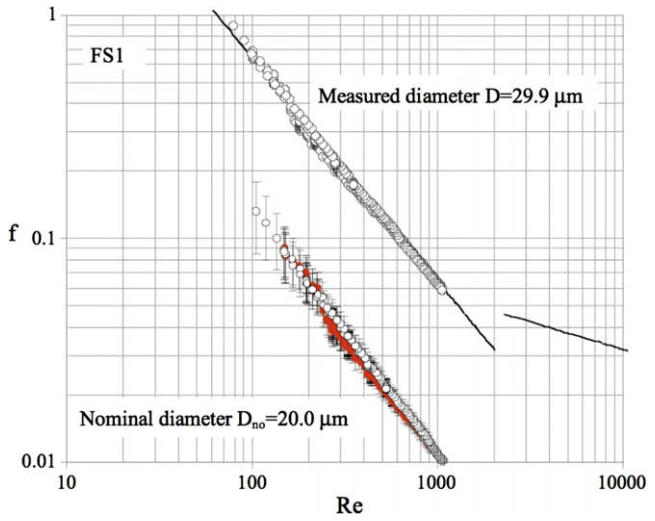

Fig. 4. Friction factor for micropipe FS1 using the nominal and the actual diameter.

tests involving micropipes. In the following figure the friction factor is always evaluated using the pipe diameter measured from SEM images, and reported in Table 2.

Friction factors (always evaluated according to the Darcy-Weisbach definition) obtained for smooth and rough micropipes in laminar regime and plotted in Fig. 4 on the Moody diagram are compared with the Poiseuille law, showing a good agreement. Nonetheless, the bi-logarithmic diagram tends to minimize differences between data and predictions. That is why we have calculated the following parameter, C^*, as:

$$C^* = \frac{fRe}{64} \tag{3}$$

i.e., the ratio between the Poiseuille number (fRe) and the theoretical value of the Poiseuille number for non-compressible laminar flow, equal to 64. The parameter C^* is plotted in Fig. 5 as a function of the Reynolds number. For a better reading only the error bars of the FS2 microtube have been plotted: for this pipe the uncertainty in the Poiseuille number ranges from ±9% ($Re > 500$) to ±59% ($Re = 30$). The uncertainty is higher for the lower Reynolds number due to the largest error associated with the gas flow rate measurement, thus explaining the general data scatter for $Re < 90$. In the range $90 < Re < 1300$ the agreement between experimental data and predictions is well within the experimental uncertainty. On the contrary, for $Re > 1300$–1500, especially for the smallest micropipes, the experimental values show and increase of the Poiseuille number with the Reynolds number. This tendency is not related to an earlier laminar-to-turbulent transition, but to the compressibility of the fluid; in fact, the friction factor continues to decrease with the Reynolds number in this range, but with a smaller slope than for the Poiseuille law, and the minimum value it reaches before starting to increase is chosen as its critical limit. When the Reynolds number increases the average fluid velocity increases too, as well as the Mach number. The fluid is accelerated by the fluid density decrease along the flow direction. The velocity gradient at the wall increases and thus the friction factor increases as well. As theoretically demonstrated by Asako et al. (2005) and by Li et al. (1999), the Poiseuille number in the laminar regime tends to increase with the pipe average Mach number when the latter becomes higher than 0.3. In the case of small diameter micropipes the Mach number can easily be higher than 0.3 for relatively small values of the Reynolds number, making compressibility effects evident, as indicated in Fig. 5.

Fig. 5 shows that for rough micropipes (SS1 and SS2) the increase of the Poiseuille number with the Reynolds number is less evident than for smooth micropipes. Needless to say that rough micropipes (stainless steel) have a larger diameter than smooth pipes; therefore, for a fixed Reynolds number rough tubes will exhibit a smaller Mach number. Consequently, in the laminar regime ($0 < Re < 2000$), compressibility effects are less important for microtubes with an inner diameter larger than 200 μm.

The data plotted in Fig. 5 show that the agreement with the classical theory is good even for rough microtubes. This would lead to conclude that friction factor in laminar flow can be considered independent of the micropipe relative roughness, up to $\varepsilon/D < 1\%$. All this is quite in agreement also with theoretical findings by Gamrat et al. (2008) and by Croce et al. (2007).

4.2. Laminar-to-turbulent transition

Experimental data of the friction factor in the transition region ($1500 < Re < 6500$) are plotted in Fig. 6 (Moody diagram) and compared with the Poiseuille law (smooth pipe, laminar regime) and the Blasius equation (smooth pipe, turbulent regime). The fluid dynamics characteristics of the DIENCA facility has allowed to run tests in the transition region only for micropipes FS2, PS2, FS3, SS1 and SS2.

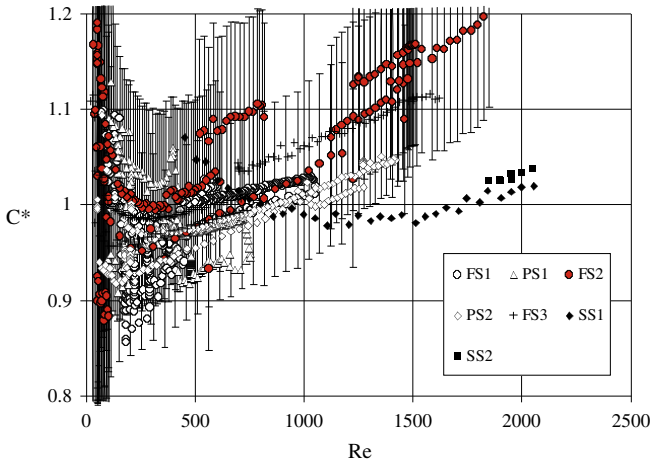

Fig. 5. The coefficient C^* defined in Eq. (3) as a function of the Reynolds number.

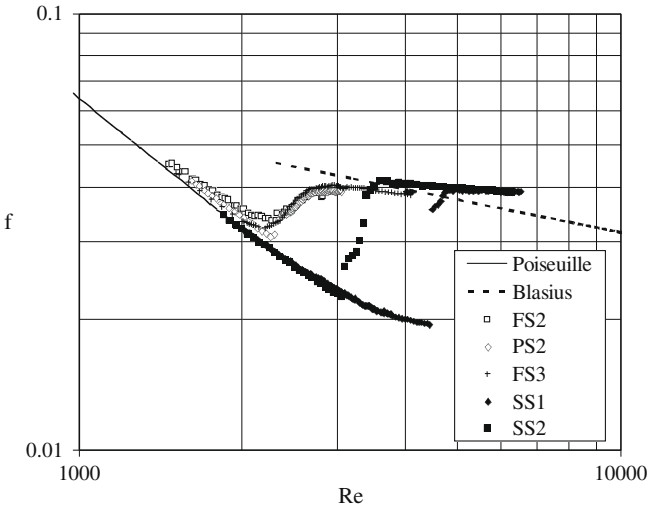

Fig. 6. Friction factor as a function of the Reynolds number in the transition region.

Colebrook (1939) published a work on the formula for friction factor in the transitional zone between laminar and fully turbulent flow (where the pressure drop would be proportional to the mean velocity squared), an account and discussion of which is given in Morini et al., 2008. The correlation which was proposed was not experimental in nature, but resulted from physico-mathematical reasoning and recognition that the friction factor could be expressed in the transitional region by a linear combination of their expressions in the turbulent and laminar regimes. Data from classes of pipes (from 2 in., i.e., 50.8 mm, up) were then considered to obtain the corresponding value of ε, which is not a roughness as normally understood in mechanical engineering, but rather the average of the values of a quantity of physical significance (the displacement from the actual pipe diameter inwards, which corresponds to the effect of roughness in conventional pipes), which was used to correlate data on a $(\lambda)^{-0.5} - Re^{*}$ plot. Thus, ranges of values for ε were given within each class of tested pipes (by experiments of several researchers), which also explains why this parameter could effectively be employed in the design phase without any need to physically measure the surface morphology of the pipes actually employed.

As outlined in Morini et al. (2007) we can expect two different type of transition in microscale:

- Smooth laminar-to-turbulent transition (ST), where the transition occurs progressively.
- Abrupt laminar-to-turbulent transition (AT), where the transition occurs in a sharp way.

As far as the first type of transition, ST, it is possible to associate the end of the laminar region and the beginning of the fully developed turbulent flow with the minimum and the maximum of the friction factor, respectively, when the fluid is subjected to the gradual passage from one flow regime to another. Conversely, for the case of abrupt transition, the zone of variation appears very narrow in the Moody diagram, and the Reynolds number at which the friction factor reaches its minimum is again chosen as the critical value.

It was Schiller (1922, quoted in e.g., Richter,1971) who reported the presence of these two different modes of transition depending on the entrance length and on the shape of the entrance (in summary: the longer the entry length the sharper the transition, which was also influenced by the kind of disturbances that the entry section introduces, the higher the disturbance the earlier the transition). A point of difference is that experiments in the case of microchannels were conducted keeping the mass flow rate constant, whereas in the case of Schiller and of the works contemporary to it, it was the pressure difference between inlet and outlet which was kept constant. In the case of an intrinsically unsteady phenomenon as flow transition, the two modes are not equivalent, but in this case they produce similar results. An experimental campaign is planned to test different forms of the inlet section to ascertain a possible influence on transition. Experimental data plotted in Fig. 6 show that the laminar-to-turbulent transition occurs at $Re > 2100$ for all micropipes. This result is in good agreement with previous data of the authors (Morini et al., 2006, 2007) and with observations for conventional pipes. As to the latter point, Richter (1971) gives an account of the critical Reynolds numbers achieved in conventional pipes, which can be considerably higher depending on how careful experimental conditions are in avoiding disturbances, but never fall below 2000, which is the value which should be taken as lower bond for conventional pipes.

Concerning the different types of transition, it can be further said that smooth micropipes (FS2, PS2 e FS3) exhibited a smooth transition, with a continuous increase in the friction factor at the increase of the Reynolds number. The critical Reynolds numbers for these pipes are 2270 (FS2), 2290 (PS2) and 2160 (FS3). As shown in Fig. 6, the behaviour of the three pipes during transition is quite similar.

As one can expect, stainless steel micropipes have shown a sudden transition occurring at higher values of the Reynolds number, namely 4430 for SS1 and 3050 for SS2. These results would seem to be in disagreement with the observation that in rough pipes the transition is usually anticipated because the roughness makes the detachment of the boundary layer at the wall easier. It is however necessary to say that in this case microtube relative roughness is limited (<1%) and that an abrupt transition has been also observed in smooth microchannels (Morini et al., 2006).

Critical Reynolds numbers obtained in previous works with rough (Morini et al., 2007) and smooth pipes (Morini et al., 2006) are plotted in Fig. 7 along with current results as a function of L/D. All rough microtubes are characterized by a relative roughness smaller than 5%, with an inner diameter from 100 to 750 μm; Reynolds number values range from 2100 to 4432. Looking at Fig. 7a we can see how rough microtubes have critical Reynolds numbers that are always smaller than smooth micropipes, where they are always higher than 2000. Fig. 7b shows how the abrupt transition (AT) tends to occur when the critical Reynolds number is large ($Re_c > 2400$). On the contrary, when the transition is characterized by comparatively small values of the critical Reynolds number, it tends to be gradual (ST). Besides, when L/D decreases both for smooth pipe and rough pipes, a large scatter in the data is present.

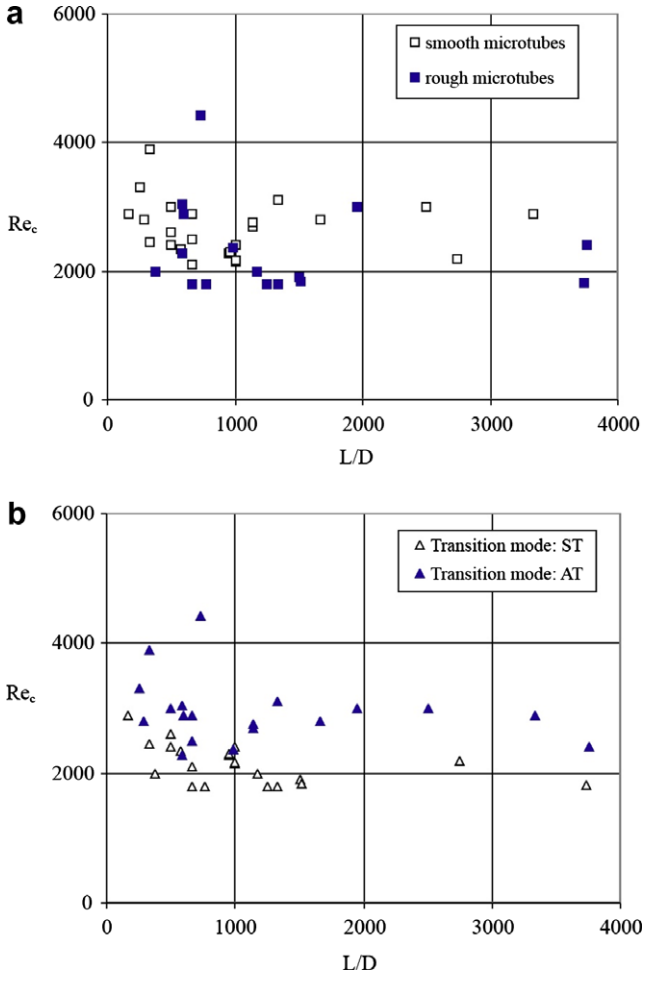

Fig. 7. Critical Reynolds number as a function of L/D: influence of roughness (a) and transition type (b).

Schiller (1922) supplied for conventional pipes a curve giving the critical Reynolds number as a decreasing function of the *L/D* ratio: only for *L/D* > 1300 is the critical value of the Reynolds number 2320, at e.g., L/D = 150 a value of 9000 was obtained. In this respect, the measurements by Kohl et al. (2005) are in line with the former findings (which were fiercely opposed by Prandtl and Tietjens (1934), who denied any dependence of the critical Reynolds number on *L/D*). In the paper by Kohl compressibility was not defined as such, but equations for friction factor for compressible flow were used for the experiments in air; as a consequence the dependence of Re_c on *L/D* cannot be related to compressibility.

4.3. Turbulent regime

The DIENCA facility has allowed to test a fully developed turbulent regime only for FS3, SS1 e SS2 microtubes.

The Poiseuille number for microtube FS3 is plotted in Fig. 8, as a function of the Reynolds number, showing a good agreement with the Blasius law.

Friction factor obtained for tubes SS1 and SS2 for *Re* > 4500 are plotted in Fig. 9 as a function of the Reynolds number. The agreement with the Colebrook correlation, valid for commercial, rough pipes of larger diameter, see Colebrook (1939), is not good, and the friction factor seems to be independent of the Reynolds number. Experimental data are lower than the corresponding Colebrook curves and show a very weak dependence on the Reynolds number. This discrepancy can be explained considering that the resistance law is not only affected by the size of the asperities but also by their shape. The surface morphology of tested microtubes is shown in Fig. 10, where SEM images are typical of all test sections used in the present study.

The distribution of the peaks around the perimeter is random, with cavities developing mainly in the longitudinal direction. This type of roughness is not typical of conventional size pipes, where cavities and peaks are randomly distributed along the axial direction. Such a distribution justified the simulation of roughness constructed by Nikuradse using sand grains. Besides, as observed by Kandlikar et al. (2005), the Colebrook correlation has been obtained from experiments carried out with sixteen tubes, the diameter of which was ranging from 101.6 mm up to 1524 mm, with an average roughness between 0.043 mm and 0.254 mm. Because of this it could be reasonable that the Colebrook correlation may be inadequate in describing the friction factor behaviour in turbulent flow in microtubes, and might be necessary to modify it for a better prediction.

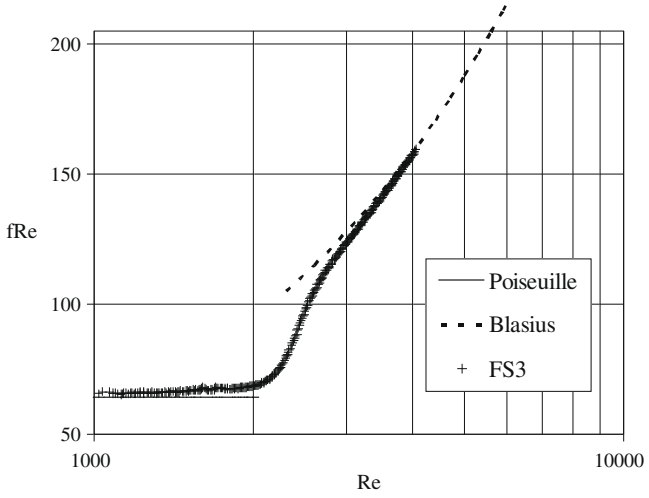

Fig. 8. Poiseuille number as a function of the Reynolds number for FS3 micropipe.

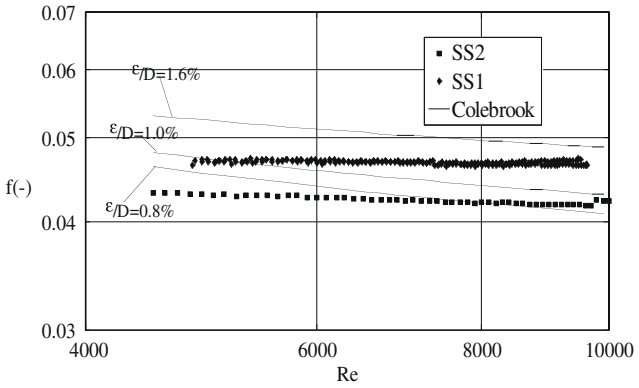

Fig. 9. Friction factor as a function of the Reynolds number in turbulent regime (stainless steel pipes).

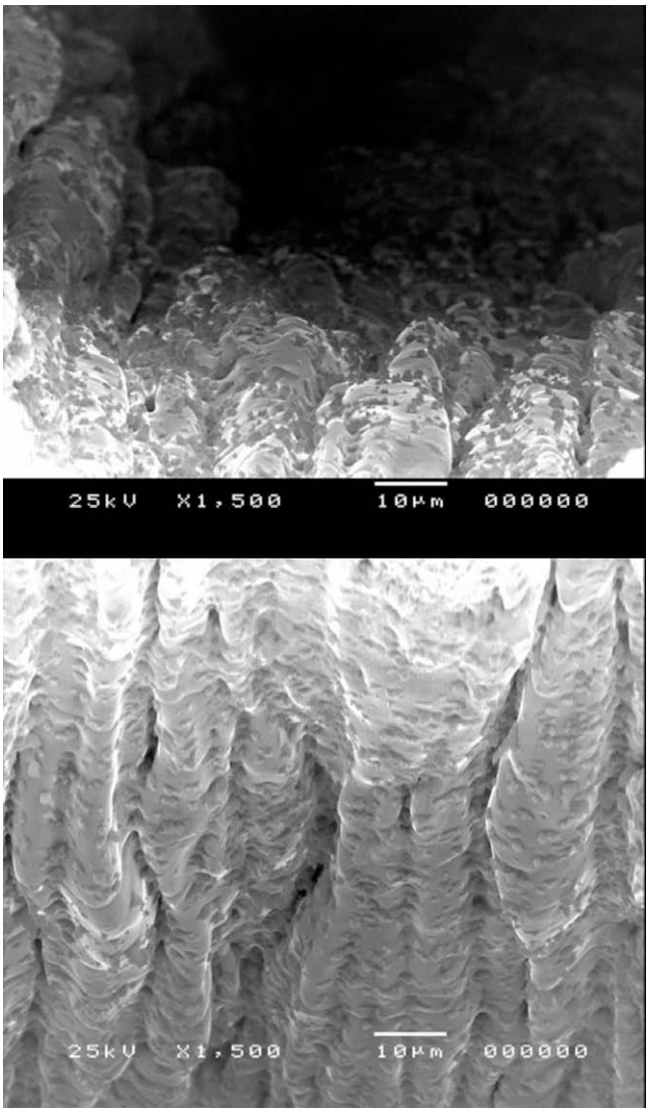

Fig. 10. Details of surface roughness of stainless steel commercial microtubes.

It is well known that surface irregularities characterised by a reduced wavelength and relatively high amplitude, which is the case of micropipes, gives rise to a friction factor in turbulent flow which is almost independent of the Reynolds number though very sensitive to the relative roughness (ε/D), just as experimental data

plotted in Fig. 9 would seem to confirm. This means that, for rough commercial micropipes the flow resistance in turbulent flow tends to become proportional to the average fluid velocity squared.

5. Conclusions

The present work reports on an experimental research on compressible fluid flow in rough and smooth micropipes with inner diameter from 29 to 508 μm. The main conclusions can be summarized as follows:

- the benchmark between two different facilities in two different laboratories has provided a good similarity of data and a good agreement with classical correlations;
- in laminar flow the agreement with the conventional theory (for large pipes) is excellent both for smooth and rough microtubes ($\varepsilon/D < 1\%$);
- for the smallest diameter micropipes ($D < 100$ μm) when $Re > 1300$ the friction factor tends to deviate from the Poiseuille law; this is caused by the acceleration associated with compressibility effect;
- there is no evidence of an early transition, with respect to conventional size pipes; the critical Reynolds number for the transition ranges from 2160 to 4430;
- both smooth (ST) and abrupt transitions (AT) have been experienced, the latter being the one the prevailing when the critical Reynolds number is larger than 2400;
- no demonstrable dependence of the critical Reynolds number on L/D has been detected;
- in developing turbulent flow the flow resistance appears to be proportional to the average fluid velocity squared and therefore in disagreement with available correlations for rough pipes (Colebrook); this could be explained considering the difference in shape and distribution of roughness in microtubes with respect to large pipes.

References

Acosta, R.E., Muller, R.H., Tobias, W.C., 1985. Transport processes in narrow (capillary) channels. AIChE Journal 31, 473–482.

Asako, Y., Nakayama, K., Shinozuka, T., 2005. Effect of compressibility on gaseous flows in a micro-tube. Int. J. Heat Mass Transfer 48, 4985–4994.

Celata, G.P., Cumo, M., McPhail, S.J., Tesfagabir, L., Zummo, G., 2006. Experimental study on compressible flow in microtubes. Int. J. Heat Fluid Flow 28, 28–36.

Choi, S.B., Barron, R.F., Warrington, R.O., 1991. Fluid flow and heat transfer in microtubes. In: Micromechanical Sensors, Actuators and Systems, ASME DSC 32, Atlanta, GA, pp. 123–134.

Colebrook, F.C., 1939. Turbulent flow in pipes with particular reference to the transition region between the smooth and rough pipe laws. J. Inst. Civ. Eng. Lond. 11, 133.

Croce, G., D'Agaro, P., Nonino, C., 2007. Three-dimensional roughness effect on microchannel heat transfer and pressure drop. Int. J. Heat Mass Transfer 50, 5249–5259.

Faghri, M., Turner, S.E., 2003, Gas flow and heat transfer in microchannels. In: Proceedings of SAREK Summer Annual Conference, Muju, Korea, pp. 542–550.

Gamrat, G., Favre-Marinet, M., Le Person, S., Baviere, R., Ayela, F., 2008. An experimental study and modelling of roughness effects on laminar flow in microchannels. J. Fluid Mech. 594, 399–423.

Hetsroni, G., Mosyak, A., Pogrebnyak, E., Yarin, L.P., 2005. Fluid flow in microchannels. Int. J. Heat Mass Transfer 48, 1982–1998.

Hrnjak, P., Tu, X., 2007. Single phase pressure drop in microchannels. Int. J. Heat Fluid Flow 28, 1–14.

Kandlikar, S.G., Schmitt, D.J., Carrano, A.L., Taylor, J.B., 2005. Characterization of surface roughness effects on pressure drop in single-phase flow in minichannels. Phys. Fluids, 17 (100606-100606-11).

Kohl, M.J., Abdel-Khalik, S.I., Jeter, S.M., Sadowski, D.L., 2005. An experimental investigation of microchannel flow with internal pressure measurements. Int. J. Heat Mass Transfer 48, 1518–1533.

Kurokawa, J., Morikawa, M., 1986. Accelerated and decelerated flows in a circular pipe. Bull. JSME 29, 758–765.

Li, Z.X., Xia, Z.Z., Du, D.X., 1999, Analytical and experimental investigation on gas flow in a microtube. In: Proc of Kyoto University-Tsinghua University Joint Conference on Energy and Environment, Kyoto, Japan, pp. 1–6.

Li, Z.X., Du, D.X., Guo, Z.Y., 2000, Experimental study on flow characteristics of liquid in circular microtubes. In: Celata, G.P., et al. (Eds.), Proc. of International Conference on Heat Transfer and Transport Phenomena in Microscale, Begell House, New York, USA, pp. 162–168.

Lorenzini, M., Morini, G.L., Henning, T., Brandner, J.J., 2007, Experimental uncertainties analysis as a tool for friction factor determination in microchannels. In: Proceedings of 4th International Conference on Microchannels and Minichannels, Puebla, Mexico.

Moffat, R.J., 1988. Describing the uncertainties in experimental results. Exp. Therm. Fluid Sci. 1, 3–17.

Morini, G.L., 2004a. Single-phase convective heat transfer in microchannels: a review of experimental results. Int. J. Thermal Sci. 43, 631–651.

Morini, G.L., 2004b. Laminar-to-turbulent flow transition in microchannels. Microscale Thermophys. Eng. 8, 15–30.

Morini, G.L., Lorenzini, M., Salvigni, S., 2006. Friction characteristics of compressible gas flows in microtubes. Exp. Therm. Fluid Sci. 30, 733–744.

Morini, G.L., Lorenzini, M., Colin, S., Geoffroy, S., 2007. Experimental analysis of pressure drop and laminar to turbulent transition for gas flows in microtubes. Heat Transfer Eng. 28, 670–679.

Morini, G.L., Lorenzini, M., Berthellemy, P., Spiga, M., 2008. Pressure drop in transitional and turbulent regime for isothermal gas flows through microtubes. In: First European Conference on Microfluidics (MicroFlu'08), Bologna (CD-rom).

Obot, N.T., 2002. Toward a better understanding of friction and heat/mass transfer in microchannels – a literature review. Microscale Thermophys. Eng. 6, 155–173.

Peng, X.F., Peterson, G.P., 1996. Forced convection heat transfer of single-phase binary mixtures through microchannels. Exp. Therm. Fluid Sci. 12, 98–104.

Richter, H., 1971. Rohrhydraulik. Springer. pp. 103–113.

Prandtl, L., Tietjens, O.G., 1934. Applied Hydro- and Aeromechanics. Dover Publications, Inc.. pp. 40–46.

Schiller, L., 1922. Investigations on laminar and turbulent flow. Z. Angew. Math. Mech. 2, 96.

Schwartz, L.W., 1987. A perturbation solution for compressible viscous channel flows. J. Eng. Math. 21, 69–86.

Shapiro, A.K., 1953. The dynamics and thermodynamics of compressible fluid flow, vol. 1–2. John Wiley.

Stanley, R.S., Barron, R.F., Ameel, T.A., 1997. Two-phase flow in microchannels. In: Proceedings of Micro electro mechanical Systems (MEMS) (DSC/ASME n 62), pp. 143–152.

Tang, G.H., He, Y.L., 2004. An experimental investigation of gaseous flow characteristics in microchannels. In: Proceedings of Second International Conference on Microchannels and Minichannels, Rochester, pp. 359–366.

Tang, G.H., Li, Z., He, Y.L., Tao, Q.W., 2007. Experimental study of compressibility, roughness and rarefaction influences on microchannel flow. Int. J. Heat Mass Transfer 50, 2282–2295.

Vijayalakshmi, K., Anoop, K.B., Patel, H.E., Harikrishna, P.V., Sundararajan, T., Das Sarit, K., 2009. Effects of compressibility and transition to turbulence on flow through microchannels. Int. J. Heat Mass Transfer 52, 2196–2204.

Wu, P., Little, W.A., 1983. Measurement of friction factors for the flow of gases in very fine channels used for microminiature Joule–Thompson refrigerators. Cryogenics 23, 273–277.

Yang, C.Y., Chien, H.T., Lu, S.R., Shyu, R.J., 2000. Friction characteristics of water, R-134a and air in small tubes. In: Celata G.P., et al. (Eds.), Proceedings of International Conference on Heat Transfer and Transport Phenomena in Microscale, Begell House, New York, USA, pp. 168–174.

Yu, D., Warrington, R.O., Barron, R., Ameel, T., 1995. An experimental and theoretical investigation of fluid flow and heat transfer in microtubes, In: Proceedings of ASME/JSME Thermal Engineering Joint Conference, Maui, HI, pp. 523–530.